HHS Public Access

Author manuscript

J Orthop Res. Author manuscript; available in PMC 2016 February 01.

Published in final edited form as:

J Orthop Res. 2015 February ; 33(2): 174–184. doi:10.1002/jor.22749.

Mesenchymal Stem Cell Expression of Stromal Cell-Derived Factor-1β Augments Bone Formation in a Model of Local Regenerative Therapy

Samuel Herberg[1], **Galina Kondrikova**[2,3], **Khaled A. Hussein**[4], **Maribeth H. Johnson**[5,6], **Mohammed E. Elsalanty**[4,6], **Xingming Shi**[6,7,8], **Mark W. Hamrick**[2,6,7], **Carlos M. Isales**[6,7,8], and **William D. Hill**[2,3,6,7]

[1]Department of Biomedical Engineering, Case Western Reserve University, Cleveland, Ohio

[2]Department of Cellular Biology and Anatomy, Georgia Regents University, 1459 Laney Walker Blvd., CB-1119, Augusta, Georgia 30912

[3]Charlie Norwood VA Medical Center, Augusta, Georgia

[4]Department of Oral Biology, Georgia Regents University, Augusta, Georgia

[5]Department of Biostatistics and Epidemiology, Georgia Regents University, Augusta, Georgia

[6]Institute for Regenerative and Reparative Medicine, Georgia Regents University, Augusta, Georgia

[7]Department of Orthopaedic Surgery, Georgia Regents University, Augusta, Georgia

[8]Department of Neuroscience and Regenerative Medicine, Georgia Regents University, Augusta, Georgia

Abstract

Bone has the potential for spontaneous healing. However, this process often fails in patients with co-morbidities requiring clinical intervention. Numerous studies have revealed that bone marrow-derived mesenchymal stem/stromal cells (BMSCs) hold great potential for regenerative therapies. Common problems include poor cell engraftment, which can be addressed by irradiation prior to transplantation. Increasing evidence suggests that stromal cell-derived factor-1 (SDF-1) is involved in bone formation. However, osteogenic contributions of the beta splice variant of SDF-1 (SDF-1β), which is highly expressed in bone, remain unclear. Using the tetracycline (Tet)-regulatory system we have shown that SDF-1β enhances BMSC osteogenic differentiation in vitro. Here we test the hypothesis that SDF-1β augments bone formation in vivo in a model of local BMSC transplantation following irradiation. We found that SDF-1β, expressed at high levels in Tet-Off-SDF-1β BMSCs, augments the cell-mediated therapeutic effects resulting in enhanced bone formation, as evidenced by ex vivo μCT and bone histomorphometry. The data demonstrate the specific contribution of SDF-1β to BMSC-mediated bone formation, and validate the

Correspondence to: William D. Hill (T: +1-706-721-2019; F: +1-706-721-6839); whill@gru.edu.

This work was performed at the Augusta Veterans Affairs Medical Center and Georgia Regents University.

Conflicts of interest: None.

feasibility of the Tet-Off technology to regulate SDF-1β expression in vivo. In conclusion, SDF-1β provides potent synergistic effects supporting BMSC-mediated bone formation and appears a suitable candidate for optimization of bone augmentation in translational protocols.

Keywords

irradiation; BMSCs; stem cell transplantation; bone formation; SDF-1/CXCL12

Bone possesses the ability to heal spontaneously restoring function without significant scarring following injury. However, this regenerative process fails in patients with large bone defects (e.g., due to trauma, tumors, nonunion, etc.) or impaired wound healing, resulting in the need for clinical intervention.[1] Mounting evidence suggests that bone marrow-derived mesenchymal stem/stromal cells (BMSCs) hold great promise for regenerative therapies in the musculoskeletal system.[2] The controlled delivery of BMSCs is generally perceived as a safe procedure, which has set the stage for the rapidly increasing number of clinical trials that use ex vivo expanded cell populations.[3]

The rationale for the use of BMSCs in cell therapy protocols is three-fold. First, BMSCs are capable of differentiating into osteoprogenitors and osteoblasts.[4] Second, BMSCs can suppress the host inflammatory response aiding in their post-transplantation survival.[5] Third, the ability of implanted BMSCs to secrete trophic/paracrine factors confers anti-apoptotic and chemoattractive characteristics, among others.[6] It has been postulated that BMSCs function as signaling centers to orchestrate and organize the multifaceted host response to the injury. To that end, it appears reasonable that indirect actions of implanted BMSCs may be as important in bone tissue regeneration as their direct osteogenic potential, which could lead to novel therapeutic approaches in the treatment of musculoskeletal diseases and injuries.[7,8]

Stromal cell-derived factor-1 (SDF-1)/CXCL12 is a member of the pro-inflammatory CXC chemokine family.[9] Six identified human isoforms are derived from the same gene by alternative splicing, with SDF-1α and SDF-1β being the most abundant.[10] SDF-1 and its main G-protein-coupled CXC chemokine receptor 4 (CXCR4) are widely expressed in postnatal tissues. The most important sources are the bone marrow (BM)-, lymph node-, muscle-, and lung-derived fibroblasts.[11–13] Binding of SDF-1 to CXCR4 initiates diverse downstream signaling processes,[14] including the chemotactic recruitment of regenerative cells to injury sites during the acute phase of bone healing.[15–17] Increased ectopic bone formation in transplants containing SDF-1-overexpressing BMSCs was demonstrated in an early report.[18] However, the authors found no correlation with in vitro mineralization or the expression of various bone-associated genes and concluded that the beneficial effects of SDF-1 in vivo were indirect.[18] We and others have reported a direct regulatory role of SDF-1 signaling in bone morphogenetic protein-2 (BMP-2)-induced osteogenic differentiation of mesenchymal cells in vitro[19–21] and in vivo[22–26] using ectopic and orthotopic bone formation models. Collectively, these data suggest that CXCR4 may act as a critical signaling component necessary for bone formation.

Recently, we described genetically engineered BMSCs that conditionally overexpress SDF-1β using the tetracycline (Tet)-regulatory system (Tet-Off-SDF-1β). [21] SDF-1β was chosen over the more abundant splice variant SDF-1α due to its greater resistance to proteolytic cleavage conferred by its additional 4 C-terminal amino acids relative to SDF-1α.[21,27–29] We showed that, independent of SDF-1α, SDF-1β enhances mineralization and expression of key osteogenic markers, and modulates BMP-2 signal transduction and BMSC survival under oxidative stress through increasing autophagy in vitro.[21,30]

The objective of this study was to investigate BMSC-mediated new bone formation in skeletally mature C57BL/6J male mice following irradiation preconditioning, previously shown to be permissive for BMSC engraftment following local transplantation.[8] Here, we tested the hypothesis that SDF-1β, expressed at high levels in genetically engineered Tet-Off-SDF-1β BMSCs,[21] augments endogenous bone formation in a model of direct intramedullary tibial transplantation.

MATERIALS AND METHODS

Animals

C57BL/6J male mice were purchased from Jackson Laboratories (Bar Harbor, ME). Animals were maintained at the Laboratory Animal Services research facility at Georgia Regents University and used at the age of 6 months. All aspects of the research were conducted in accordance with the guidelines set by the Georgia Regents University Institutional Animal Care and Use Committee following an approved Animal Use Protocol (protocol number 2011–0397).

Isolation and Culture of BMSCs

Six 18-month-old male C57BL/6J mice, purchased from the National Institute on Aging (Bethesda, MD) aged rodent colony, were used to obtain BMSCs at the Georgia Regents University Stem Cell Core Facility as described previously.[8,21,30–32] First, mice were euthanized by CO_2 overdose followed by thoracotomy. The femora and tibiae were dissected free of soft tissues, cut open at both ends, and flushed with complete isolation media (CIM) (RPMI-1640 (Cellgro, Mediatech, Manassas, VA), 9% heat-inactivated fetal bovine serum (FBS), 9% horse serum (both from Atlanta Biologicals, Lawrenceville, GA), and 12 μM l-glutamine (Gibco, Invitrogen, Carlsbad, CA) using a 22-gauge syringe followed by filtration through a 70 μm nylon mesh filter. The combined whole bone marrow aspirate was dispersed with a 25-gauge syringe to produce a single cell suspension. Next, BMSCs were isolated using a modified protocol[33–35] by plating the single cell suspension in 175-cm^2 flasks at a density of 2×10^7 cells/flask. After a 3 h incubation at 37°C in 5% CO_2, the nonadherent cells were removed and the adherent cells washed two times gently with PBS to reduce the degree of hematopoietic lineage cell contamination. The cells were cultured in CIM for 3–4 weeks with media change every 3–4 days. At 70–80% confluence, the cells were lifted with trypsin/EDTA, washed, and resuspended at a density of 5×10^6 cells/ml in PBS containing 0.5% bovine serum albumin (BSA) and 2 mM EDTA followed by negative immunodepletion using magnetic microbeads conjugated to anti-mouse CD11b, CD45R/B220 (BD Biosciences Pharmingen, San Diego, CA), CD11c, and PDCA-1

(Miltenyi Biotec, Bergisch Gladbach, Germany) monoclonal antibodies according to the manufacturer's instructions. Resulting CD11b, CD45R/B220, CD11c, PDCA-1-negative cells were subjected to positive immunoselection using anti-Sca-1 microbeads (Miltenyi Biotec) following the manufacturer's recommendations. Enriched BMSCs (0.33% CD45, 0.13% CD11b, 83.18% Sca-1 by FACS analysis[31]), which are depleted of monocytes, granulocytes, macrophages, myeloid-derived dendritic cells (DCs), natural killer cells, B-1 cells, B lymphocytes, T lymphocytes, classical DCs, plasmacytoid DCs, and macrophage progenitors, were maintained in Dulbecco's Modified Eagle Medium (DMEM; Cellgro) with 10% heat-inactivated FBS (Atlanta Biologicals). Next, BMSCs were subjected to retroviral-mediated transduction with ΔU3-GFP plasmid DNA, constructed in the replication defective ΔU3nlsLacZ vector by inserting the full-length coding region of *Gfp* cDNA.[32] BMSCs were seeded at low density for clonal selection. Well-isolated, GFP-positive BMSCs (clone 2) were maintained in DMEM supplemented with 10% heat-inactivated FBS and used at 70–80% confluence.

Genetic Modification of BMSCs for Conditional Expression of SDF-1β

Next, BMSCs (passage 10) were transduced with retroviral Tet-Off expression vectors as previously described.[21,30] A sequential protocol of retrovirus production, two-step infection, and selection was utilized to generate double-stable Tet-Off-SDF-1β and Tet-Off-EV (empty vector) BMSCs. Briefly, 293GPG packaging cells[36] were transfected at passage 8 with retroviral Tet-Off expression vectors containing the full-length coding sequence of murine *Sdf-1β* (NM_013655) or empty control (Clontech Laboratories, Mountain View, CA). BMSCs (clone 2) were infected at passage 10 with 2 ml of the respective retroviral supernatant containing 4 μg/ml polybrene (Sigma–Aldrich) and 100 ng/ml doxycycline (Dox; Sigma–Aldrich) followed by selection with 400 μg/ml G418 (MP Biomedicals, Solon, OH) and 2.5 μg/ml puromycin (Sigma–Aldrich). Clonally selected, genetically engineered BMSCs were maintained in DMEM supplemented with 10% Tet-FBS (Clontech), 400 μg/ml G418, and 2.5 μg/ml puromycin.

Quantitative Reverse Transcription-Polymerase Chain Reaction (qRT-PCR)

qRT-PCR analyses were performed as described previously.[8,21] Briefly, Tet-Off BMSCs (passage 16) were plated at 2.5×10^3 cells/cm^2 in 12-well plates and then treated with 100 ng/ml Dox starting the next day. After 24 h, cells were lysed in TRIzol® reagent (Invitrogen) for RNA isolation and subsequent cDNA synthesis (iScript™ kit; Bio-Rad, Hercules, CA). One hundred nanograms of cDNA were amplified in duplicates in each 40-cycle reaction using an iCycler™ (Bio-Rad) with annealing temperature set at 60°C, ABsolute™ QPCR SYBR® Green Fluorescein Mix (ABgene, Thermo Fisher Scientific), and custom-designed primers (Table 1; Thermo Fisher Scientific). A melt curve was used to assess the purity of amplification products. mRNA levels were normalized to β-actin and gene expression was calculated as fold change using the comparative C_T method.

SDF-1α and SDF-1β Enzyme-Linked Immunosorbent Assay (ELISA)

SDF-1 splice variant-specific ELISAs (R&D Systems, Minneapolis, MN) were performed as previously described.[8,21] Briefly, Tet-Off BMSCs were plated and treated as above. After 24

h, the media were collected and cell lysates prepared in Complete Lysis-M EDTA-free buffer containing protease inhibitors (Roche Diagnostics, Indianapolis, IN). The anti-SDF-1 capture antibody (R&D Systems) in sodium bicarbonate buffer pH 9.4 was bound to MaxiSorp™ 96-well plates (Nunc, Thermo Fisher Scientific) overnight. Plates were blocked for 2 h with 1% BSA in PBS. Murine SDF-1α or SDF-1β (PeproTech, Rocky Hill, NJ) standards and samples (1:2 diluted) were incubated for 2 h prior to incubating with the biotinylated anti-SDF-1α and anti-SDF-1β detection antibody (2 h; R&D Systems), respectively. Streptavidin-horseradish peroxidase (R&D Systems) was incubated for 20 min followed by the substrate reagent (R&D Systems) for 20 min. Sulfuric acid (2 N) was added to stop the enzymatic color reaction and absorbance was read at 450 nm. SDF-1α and SDF-1β protein expression was calculated using standard curves and normalized to total protein, which was quantified using the EZQ® Protein Quantitation Kit (Invitrogen).

Osteogenic Differentiation

Osteogenic differentiation was performed as described previously.[21,37] Briefly, Tet-Off BMSCs were plated at 5.0×10^3 cells/cm^2 in 12-well plates and treated as above. Starting the next day, BMSCs were incubated in standard osteogenic induction medium comprised of DMEM supplemented with 5% Tet-FBS, 0.25 mM ascorbic acid (Sigma–Aldrich), 0.1 μM dexamethasone (Sigma–Aldrich), and 10 mM β-glycerophosphate (Sigma–Aldrich) ± 100 ng/ml Dox for 21 days with daily medium exchange.

Detection and Quantification of Calcium Mineral Content

Alizarin Red S (ARS) staining was performed as described previously.[21,37] After 21 days in culture, BMSC monolayers were washed with PBS and fixed in 3% paraformaldehyde (PFA; Sigma–Aldrich) for 30 min. Cells were stained with 40 mM ARS pH 4.1 (Sigma–Aldrich) for 15 min followed by washing with excess dH_2O. Stained monolayers were visualized by scanning the plates using a conventional flatbed scanner (Canon, Melville, NY). For quantitative destaining,[38] cells were incubated for 10 min with 10% cetylpyridinium chloride (Sigma–Aldrich). Aliquots were diluted (1:10) with PBS, transferred to a 96-well plate (Nunc, Thermo Fisher Scientific, Waltham, MA), and absorbance was read at 570 nm.

Total Body Irradiation (TBI)

Twenty five 6-month-old C57BL/6 male mice received a lethal dose (8.25 Gy) of TBI at 0.825 Gy/min for 10 min using a cesium-137 source (Gammacell 40 Exactor; Best Theratronics, Ottawa, Ontario, Canada) without shielding as previously described.[8,39] This dose has been shown to result in 0% survival after 30 days in untreated mice.[40] The next day, lethally irradiated mice were anesthetized with 2% isoflourane and transplanted with 6.0×10^6 cells/ml of rescuing whole BM, obtained from femora and tibiae of donor litter mates, supplemented with 1% diprotin A to enhance BM cell engraftment[8,39,41] (Peptide Institute, Osaka, Japan) by injection into the retro-orbital sinus.

Intramedullary Tibial Transplantation

Direct intramedullary tibial transplantations were performed as described previously.[8,39] First, lethally irradiated recipient mice were anesthetized with 2% isoflourane followed by subcutaneous injection of 2.5 mg/kg carprofen for pre-surgical analgesia. The injection site was shaved and 10% betadine solution (Purdue Products L.P., CT) applied topically. The knee was flexed to 90° and the proximal end of the tibia drawn to the anterior. A 26-gauge needle was inserted into the joint surface of the tibia through the patellar tendon and then inserted into the medullary space. The needle was removed, a second 26-gauge needle inserted into the needle track, and extended into the BM space to flush with 100 μl 0.9% saline. Genetically engineered Tet-Off-SDF-1β or Tet-Off-EV BMSCs (passage 16)[21] at 1.32×10^7 cells/ml supplemented with 1% diprotin A to enhance BMSC engraftment[41] (Peptide Institute) were slowly injected into the left marrow cavity as the needle was withdrawn from the intramedullary space (70 μl; 9.24×10^5 cells total; n = 5/Tet-Off-SDF-1β (−Dox); n = 5/Tet-Off-SDF-1β (+Dox); n = 10/Tet-Off-EV). Right tibiae were injected with vehicle control (n = 5/Tet-Off-SDF-1β (−Dox); n = 5/Tet-Off-SDF-1β (+Dox); n = 10/Tet-Off-EV). Recipient mice were fed with regular animal chow and had access to antibiotic-containing water (Hi-Tech Pharmacal, Amityville, NY) for 2 days before switching to water ad libitum. Drinking water was supplemented with 5% glucose ± 25 μg/ml doxycycline (Dox; Sigma–Aldrich) for the duration of the study.[42] After 4 weeks, animals were euthanized by subcutaneous administration of a ketamine HCl (85 mg/kg; IP)/xylazine HCl (15 mg/kg; IP) cocktail followed by thoracotomy. Tibiae were removed, dissected free of soft tissues, and fixed in 3% PFA. After 24 h, specimens were washed in PBS and preserved in 70% ethyl alcohol at 4°C.

Micro Computed Tomography (μCT)

Tibiae were scanned with an ex vivo μCT system (Skyscan 1174; Skyscan, Aartselaar, Belgium) as previously described.[8] The scanner was equipped with a 50 kV, 800 μA X-ray tube and a 1.3 megapixel CCD coupled to a scintillator. Four tibiae were placed in a plastic sample holder with the long axes oriented parallel to the image plane and scanned in air using 18 μm isotropic voxels, 400 ms integration time, 0.5° rotation step, 360° rotation, and frame averaging of 5. All samples were scanned within the same container using the same scanning parameters. All scans were then reconstructed using NRecon software v1.6.6.0 (Skyscan) with exactly the same reconstruction parameters. For 3-D analysis (CTAn software v1.12.0.0 +, Skyscan), the grey scale was set from 60 to 140. This range allowed viewing of the normal bone architecture seen in the raw images. All reconstructed images were adjusted to this grey scale before running the 3-D analysis. Standard 3-D morphometric parameters[43] were determined in a region of interest (ROI) starting immediately beyond the epiphyseal plate (transaxial tracing; 112 cuts = 2 mm distally; Fig. 1) in all samples. Representative 3-D images were created using CTvox software v2.3.0 r810 (Skyscan).

Histological Preparation and Analysis

Tibiae were decalcified in 0.25 M ethylenediaminetetraacetic acid (EDTA) at pH 7.4 for 7 days at 4°C with changes of the EDTA solution every other day as described previously.[8]

Specimens were washed, dehydrated in a graded series of ethyl alcohol (70–100%), cleared in xylene, embedded longitudinally in paraffin, and sectioned at 5 μm thickness using a microtome (Leica Microsystems Inc., Buffalo Grove, IL) prior to mounting on Frost Plus glass slides for histology. Coronal sections through the center of the diaphysis were stained with standard hematoxylin & eosin (H&E) for histologic analysis. Light microscopy images were captured using a Carl Zeiss microscope (Carl Zeiss, Inc., Thornwood, NY) with AxioVision Image Analysis software v4.7.1.0.

Bone Histomorphometry

The standard 2-D histomorphometric parameter[44,45] percent bone volume (BV/TV) was assessed in the proximal tibiae (n = 3 animals/group) as described previously.[8] We utilized a 876.9 × 657.1 μm rectangular ROI (H&E-stained coronal sections through the center of the diaphysis, 20×, 1388 × 1040 pixels per image, 576211.68 μm^2 or 0.58 mm^2 combined total area in four identical quadrants; Fig. 5A). Following an established protocol,[46] black-and-white image masks of the H&E-stained color images were created using the wand tool (tolerance: 10) in Photoshop CS6 software v13.0 (Adobe Systems, San Jose, CA) to highlight areas of bone. In all 20X images, bone tissue was designated in black while the remaining tissue was designated in white, creating the mask for analysis (Fig. 6B–D). Next, using ImageJ software 1.47v (NIH; Washington, DC), the entire image area was calculated as tissue area (T.Ar) and, using the default wand tool, the combined black-colored areas were summarized as bone area (B.Ar) to calculate percent bone volume (BV/TV). Per definition, BV/TV is numerically identical with the corresponding area/area ratio B.Ar/T.Ar.[44]

Immunohistochemistry

Five-micrometer paraffin sections (coronal; through the center of the diaphysis) were deparaffinized in xylene, hydrated, and permeabilized in 0.1% TritonX100 for 10 min, as previously described.[8] Antigen retrieval was performed using the Digest-All-3 solution (Invitrogen, Carlsbad, CA). Non-specific binding was blocked using 3% normal donkey serum (Jackson Immuno Research, West Grove, PA) for 1 h at room temperature in a humidifying chamber. Serial coronal sections were incubated with primary Rb (rabbit) anti-GFP antibody (1:300; Molecular Probes, Invitrogen) overnight at 4°C. For detection of immunopositive signals, sections were incubated with Alexa Fluor® 488-conjugated secondary D (donkey) anti-Rb antibody (1:500; Jackson ImmunoResearch) for 2 h at room temperature in a humidifying chamber. Sections were cover-slipped with Vectashield mounting medium (Vector Laboratories Inc., Burlingame, CA) containing 4′,6-diamidino-2-phenylindole (DAPI) nuclear stain. Differential interference contrast (DIC) and fluorescence microscopy images were captured using a Carl Zeiss microscope with AxioVision Image Analysis software v4.7.1.0 (Carl Zeiss).

Statistical Analysis

All data are expressed as means ±SD. In vitro experiments (n = 3) were performed two independent times. Transcript and protein levels, and in vitro mineralization were analyzed using the one-way analysis of variance (ANOVA). Tibial transplantation outcomes analyzed

were 3-D bone morphometric parameters; percent bone volume (BV/TV), and trabecular number (Tb.N), thickness (Tb.Th), and separation (Tb.Sp). A two-way repeated measures ANOVA was used. The model included treatment (TRT: Tet-Off-SDF-1β [−Dox], Tet-Off-SDF-1β [+Dox], Tet-Off-EV) as the fixed effect, BMSC transplantation (BMSC: no vs. yes) as the within animal repeated random effect, and the interaction between TRT and BMSC. A significant interaction effect would infer that the TRTs had a different effect on the outcome dependent on the presence or absence of BMSCs. The bone histomorphometric parameter BV/TV was analyzed using the one-way ANOVA and non-parametric Spearman's rank correlation followed by the unpaired Student's t test. A Tukey's *post hoc* test was used to test for significant effects. The significance level was set at alpha = 0.05 and SAS© v9.3 (SAS Institute, Inc., Cary, NC) was used for all analyses.

RESULTS

SDF-1β Transcript and Protein Analysis

We first determined the levels of SDF-1β mRNA and protein expression in genetically engineered Tet-Off-SDF-1β and Tet-Off-EV BMSCs. Similar to previous studies,[21] SDF-1β mRNA levels in Tet-Off-SDF-1β BMSCs were significantly increased compared to Dox-suppressed controls (29.9 ± 7.9-fold, $p<0.0001$) (Fig. 2A), which was similar to the results seen with the Tet-Off-EV control groups (Fig. 2A). Comparable levels of SDF-1α mRNA levels were found across all groups (Fig. 2A, inset). In accordance with transcript data, intracellular SDF-1β protein levels in Tet-Off-SDF-1β BMSCs were significantly increased relative to Dox-suppressed controls (5.4 ± 0.7-fold, $p<0.0001$) (Fig. 2B). This was reflected in SDF-1β levels secreted in the culture media (7.0 ± 1.6-fold, $p<0.0001$) (Fig. 2C). No differences were seen between Tet-Off-EV control groups (Fig. 2B, C). As seen with mRNA expression, overall SDF-1α protein levels were comparable among all groups (Fig. 2B and C, insets).

In Vitro Osteogenic Differentiation

Next, we assessed the role of SDF-1β in BMSC osteogenic differentiation in vitro. Tet-Off BMSCs were cultured for 21 days in osteogenic induction medium before calcium mineral content was detected and quantified by standard Alizarin Red S (ARS) staining. SDF-1β in Tet-Off-SDF-1β BMSCs significantly enhanced osteogenic differentiation relative to Dox-suppressed controls (1.7 ± 0.3-fold, $p<0.0001$) (Fig. 2D and E). ARS staining of Tet-Off-EV control BMSCs revealed no differences between groups (Fig. 2D and E). In agreement with our previous studies,[21] this suggests that wild type-like Tet-Off-EV control BMSCs express basal levels of SDF-1α and SDF-1β under both Dox conditions, which does not affect their osteogenic differentiation potential in vitro. Hence, we included a single Tet-Off-EV BMSC group for subsequent tibial transplantation.

BMSC-Mediated New Bone Formation

In previous studies we showed that irradiation preconditioning is permissive for BMSC engraftment following direct tibial transplantation.[8] Therefore, we here investigated the specific contribution of SDF-1β over-expression to BMSC-mediated new bone formation in a model of direct tibial transplantation. Representative 3-D reconstructions of ex vivo μCT

images 4 weeks post-transplantation are depicted in Figure 3. Quantitative analyses of trabecular bone morphometric parameters in the proximal tibiae using an ROI starting immediately beyond the epiphyseal plate and extending 2 mm distally by transaxial tracing revealed significantly increased (2.2–3.1-fold, $p < 0.0001$) percent bone volume (BV/TV) in all BMSC-transplanted groups relative to vehicle controls (Fig. 4A). Importantly, tibiae transplanted with Tet-Off-SDF-1β BMSCs showed significantly greater new bone formation in comparison to Dox-suppressed and Tet-Off-EV controls (BV/TV: Tet-Off-SDF-1β (−Dox), 45.2 ± 4.9%; Tet-Off-SDF-1β (+Dox), 35.2 ± 7.9%; Tet-Off-EV, 35.0 ± 8.2%, $^{a}p < 0.05$) (Fig. 4A), inferred by a significant interaction ($p = 0.015$). Measurements of trabecular number (Tb.N, 1.9–2.7-fold, $p < 0.0001$, $^{a}p < 0.05$) showed a similar pattern (Fig. 4B) with significant interactions ($p = 0.014$, $p = 0.007$). Trabecular thickness (Tb.Th) in BMSC-transplanted groups was significantly increased relative to vehicle controls (1.1–1.2-fold, $p < 0.05$, $p < 0.0001$) (Fig. 4C); no differential effect due to treatment was observed ($p = 0.663$). Trabecular separation (Tb.Sp) was significantly decreased (0.7–0.9-fold, $p < 0.01$, $p < 0.0001$) compared to controls (Fig. 4D) with a trend towards interaction ($p = 0.056$).

Histology and Bone Histomorphometry

Qualitative histologic analysis mirrored the 3-D microstructural bone evaluation and revealed a mix of red and white (fatty) marrow with few trabeculi interspersed in vehicle controls (Fig. 5A). As reported previously, the rescuing whole BM transplant 24 h after irradiation allows for sufficient reconstitution of the BM progenitor and hematopoietic stem cell populations. Consequently, the marrow exhibited a typical composition without signs of irradiation-induced bone loss.[8] However, there was an increase in bone marrow adipocytes in all irradiated mice as previously seen.[8] Administered BMSCs across stem cell therapy groups induced significant de novo bone formation in the proximal tibiae predominantly localized along the track of injection. Trabecular bone was embedded in a cell-rich fibrovascular marrow with few mature adipocytes (Fig. 5B–D). A clear overall reduction of BM adipocytes in BMSC-transplanted tibiae was observed relative to vehicle controls. Notably, tibiae transplanted with Tet-Off-SDF-1β BMSCs suggested SDF-1β-enhanced new bone formation compared to Dox-suppressed and Tet-Off-EV controls, as evidenced by a greater density of new trabeculi (Fig. 5B–D). This was confirmed by quantitative 2-D bone histomorphometry. In agreement with the μCT data, significantly increased (3.7–6.0-fold, $p < 0.05$, $p < 0.0001$) percent bone volume (BV/TV) was observed in all BMSC-transplanted groups relative to vehicle controls (Fig. 6E). Importantly, tibiae transplanted with Tet-Off-SDF-1β BMSCs showed significantly greater amounts of trabecular bone in comparison to Dox-suppressed and Tet-Off-EV controls (BV/TV: Tet-Off-SDF-1β (−Dox), 71.0 ± 16.5%; Tet-Off-SDF-1β (+Dox), 44.3 ± 6.5%; Tet-Off-EV, 42.6 ± 6.9%, $^{a}p < 0.05$) (Fig. 6E), thereby confirming the μCT data with significant correlation between methodologies (Spearman's rank correlation coefficient $r = 0.98$, $p < 0.0001$).

Immunohistochemistry

Immunohistochemistry using a combined DIC/fluorescence microscopy approach revealed no evidence of GFP signal in the marrow of vehicle controls (Fig. 7A), thereby confirming our previous results.[8] In contrast, comparable levels of GFP-positive cells, predominantly in the marrow space and lining trabecular structures contributing to the endosteum, were

observed across all cell therapy groups (Fig. 7B–D). Furthermore, GFP-positive cells were found embedded in the trabecular bone matrix as osteocytes; however, the majority of the adjacent trabecular osteocytes were non-GFP expressing suggesting they were derived from endogenous progenitor cells (Fig. 7B–D1,2). This indicates that both the transplanted and endogenous BMSCs survived, engrafted, and contributed to new bone formation during the 4-week healing period following myeloablative injury (Fig. 7B–D). Our data also suggest that while the transplanted cells exerted limited direct involvement in new bone formation, they drove endogenous osteogenic cell-mediated bone formation via paracrine actions, and this was enhanced in SDF-1β over-expressing BMSCs. Collectively, our findings show that SDF-1β enhances the osteogenic potential of BMSCs in a model of cell therapy. Furthermore, these studies validate the feasibility of the Tet-technology to conditionally regulate the expression of SDF-1β in vivo.

DISCUSSION

The aim of the present study was to investigate BMSC-mediated new bone formation in a mouse model of local cell therapy. We tested the hypothesis that SDF-1β, expressed at high levels in genetically engineered Tet-Off-SDF-1β BMSCs, enhances cell-mediated osteogenesis. Our data suggest that transplanted BMSCs in all groups significantly increase bone formation relative to vehicle controls following irradiation preconditioning. Importantly, SDF-1β was found to augment the osteogenic potential of transplanted BMSCs. Our findings also validate the feasibility of the Tet-Off technology to conditionally regulate the expression of SDF-1β in vivo.

Previous studies have suggested that the CXCR4/SDF-1 axis functions in postnatal bone formation by regulating osteoblast development in cooperation with BMP signaling, and that CXCR4 acts as an endogenous signaling component necessary for bone formation.[25] Until recently the presence of SDF-1β in bone and osteogenic cells was poorly appreciated.[21,47] Further, we have recently shown that SDF-1β protein appears to be present at a higher level than the better studied alpha isoform.[21] Importantly, we have demonstrated that SDF-1β potentiates osteogenic differentiation and chemotaxis of CXCR4-expressing BMSCs in vitro, suggesting both autocrine and paracrine activities independent of SDF-1α.[21] The use of the Tet-Off regulatory system allows for tightly controlled trans-gene expression,[48] which results in significantly increased SDF-1β mRNA (~30-fold) and protein (~5-fold) expression levels in engineered BMSCs.[21] Hence, employing both an internal (+Dox) and external control (empty vector; +or −Dox are equivalent[21]) provides a suitable model to investigate the specific role of SDF-1β in different cell processes. The consistent, yet adjustable, cellular expression levels of SDF-1β are comparable to continuous endogenous exposure and avoid potential inconsistencies associated with exogenous preconditioning or transient genetic over-expression. SDF-1β was selected over the more abundant splice variant SDF-1α due to its greater resistance to C-terminal proteolytic cleavage and glycosaminoglycan-dependent stabilization on cell and extracellular surfaces.[27,28] This raises the possibility that SDF-1β may be better suited for local applications directly in the BM microenvironment, particularly in bone injury sites with increased inflammatory and proteolytic activity. The differential processing could provide a mechanism for fine regulation of the local and distant functional activity of SDF-1, favoring SDF-1β over SDF-1α. It appears feasible that SDF-1α with a

shorter active half-life may stimulate more acute CXCR4 signaling in the BM, whereas the more stable SDF-1β may be critical in mediating chronic effects on BMSC osteoinduction.

Conditioning by radiation is widely used in preclinical and clinical protocols to ensure successful whole BM or BMSC transplantation.[49–52] In allogeneic transplantation, irradiation also prevents the host immune response toward the graft.[53] Accumulating evidence suggests that SDF-1 is quickly upregulated in the BM in response to irradiation (~2 days), outlining the optimal time window for transplantation studies.[53–57] The increase in SDF-1 expression during injury situations is believed to be part of the host defense mechanism counteracting the effects of DNA-damaging regimens, which often result in cell death and anemia.[58,59] SDF-1 has been shown to increase the repopulation of the BM niche site following myeloablative injury by promoting the survival and proliferation of transplanted BM stem cells, including hematopoietic stem cells and BMSCs, in addition to enhancing the homing of macrophages, which aid in clearing apoptotic cells from the irradiated BM.[39,41,50,53] Furthermore, SDF-1 is known to affect migration patterns of both injected and host BMSCs as well as circulating BM-derived osteoblast progenitors.[15–17] In a recent study we showed that irradiation preconditioning is permissive for BMSC engraftment following direct tibial transplantation.[8] Importantly, the number of BMSCs transplanted was linked to the ultimate number of BMSCs that engrafted and the degree of new trabecular bone formation, which is driven in large part by the recruitment of endogenous cells.[8] The cell dose chosen here was the highest used in that study and showed maximal new bone formation. This was also the dose where the increase in new bone formation relative to the number of BMSCs transplanted plateaued. As such, the significant new bone formation shown by increasing SDF-1β expression at this cell dose is even more striking suggesting it can help optimize regenerative bone therapies. We hypothesize that BMSC engraftment occurs in the irradiated BM, in part, because intra-medullary injection permits large numbers of BMSCs to come into close physical contact with BMSC niche site cells that have been induced to express very high levels of SDF-1 on their surface, or in a narrow gradient near their surface.[26] It has been shown that at very high concentrations, SDF-1 switches the downstream CXCR4 signaling (“biased agonism”), possibly by forming dimers,[60,61] from G-protein-coupled- to β-arrestin-mediated pathways.[60,62] Consequently, that switch can cause the inhibition of cell migration, effectively retaining cells in place.[60,62] This implies that following irradiation the levels of SDF-1 on, or near, the niche cell surface is high enough to induce a switch in CXCR4 signaling and retain the locally injected BMSCs permitting their engraftment. Once successfully engrafted, BMSCs have been suggested to confer a critical positive osteogenic influence on the BM microenvironment by secreting paracrine factors to prolong the modulation of the host response. As such, these indirect actions of implanted BMSCs are thought to be as important in bone tissue regeneration as their direct osteogenic potential.[6]

Our data demonstrate that SDF-1β, expressed at high levels in Tet-Off-SDF-1β BMSCs, augments the cell-mediated therapeutic effects resulting in enhanced bone formation relative to controls, as evidenced by 3-D morphometric analysis of standard ex vivo μCT parameters,[43] histology, and bone histomorphometry.[44,45] The use of high-resolution ex vivo μCT imaging to assess bone morphology and microarchitecture in experimental studies has grown immensely in recent years.[43] Ideally, the smallest voxel size available would be

used for all scans (i.e., for our instrument 9 μm); however, this comes at the expense of significantly longer acquisition times. Here, we used voxels of 18 μm as a compromise that would still provide very good resolution of murine trabeculi, which typically have a thickness of 20–60 μm.[63] As a consequence, we are potentially on average slightly overestimating object thickness of the smallest objects in this study. However, the Tb.Th data are consistent with the BV/TV, Tb.N, and Tb.Sp measurements, and in agreement with previous results.[8] The μCT data furthermore showed excellent correlation with 2-D histomorphometry. In a relevant recent study we found no gross histological differences between irradiated and non-irradiated vehicle controls outside of increased adipogenesis,[8] suggesting that the commonly observed radiation-induced bone loss[64] was not detectable after 4 weeks in our lethal irradiation model. This is most likely due to our rescuing transplantation of whole BM shortly after lethal irradiation, which reestablishes a significant portion of the BM progenitor and hematopoietic stem cell populations, and protects some of the surviving endogenous cells.[8] Whole BM transplantation is generally not used in sub-lethal irradiation models of bone injury.[8,64] Importantly, the data support our previous in vitro[21] and in vivo[8] findings and demonstrate the specific direct contribution of SDF-1β to BMSC-mediated bone formation. We also provide in vivo proof of principle of the Tet-Off regulatory system.[48] The current study presents new evidence on the importance of SDF-1β, newly recognized to be abundant in bone, in regulating BMSC-mediated osteogenesis in situ. Together with our recent reports showing SDF-1β-mediated BMP-2 healing of critical-size calvarial defects using osteoconductive matrices for local delivery[26,37], this study supports the potential translational use of SDF-1β in bone defect repair. Future studies aim to investigate in vivo the mechanisms of SDF-1β's modulatory effects in terms of BMSC homing, capture, and osteogenic induction of transplanted as well as endogenous stem cells and osteogenic lineage cells.

Acknowledgments

This publication is based upon work supported in part by the Department of Veterans Affairs, Veterans Health Administration, Office of Research and Development, Biomedical Laboratory Research and Development Program (VA Merit Award 104462, W.D.H.) and the National Institutes of Health (NIA-AG036675-01, W.D.H.). The contents of this publication do not represent the views of the Department of Veterans Affairs, or the United States Government. The authors appreciate the technical support of Donna Kumiski and Penny Roon, Georgia Regents University Histology Core Facility.

References

1. Mountziaris PM, Mikos AG. Modulation of the inflammatory response for enhanced bone tissue regeneration. Tissue Eng Part B Rev. 2008; 14:179–186. [PubMed: 18544015]
2. Caplan AI. Why are MSCs therapeutic. J Pathol. 2009; 217:318–324. [PubMed: 19023885]
3. Steinert AF, Rackwitz L, Gilbert F, et al. Concise review: the clinical application of mesenchymal stem cells for musculoskeletal regeneration: current status and perspectives. Stem Cells Transl Med. 2012; 1:237–247. [PubMed: 23197783]
4. Pittenger MF, Mackay AM, Beck SC, et al. Multi-lineage potential of adult human mesenchymal stem cells. Science. 1999; 284:143–147. [PubMed: 10102814]
5. Krampera M, Glennie S, Dyson J, et al. Bone marrow mesenchymal stem cells inhibit the response of naive and memory antigen-specific T cells to their cognate peptide. Blood. 2003; 101:3722–3729. [PubMed: 12506037]
6. Caplan AI, Dennis JE. Mesenchymal stem cells as trophic mediators. J Cell Biochem. 2006; 98:1076–1084. [PubMed: 16619257]

7. Jones E, Yang X. Mesenchymal stem cells and bone regeneration: current status. Injury. 2011; 42:562–568. [PubMed: 21489533]
8. Herberg S, Kondrikova G, Hussein K, et al. Total body irradiation is permissive for mesenchymal stem cell-mediated new bone formation following local transplantation. Tissue Eng Part A. 2014 Jun 10. Epub ahead of print.
9. Zlotnik A, Yoshie O. Chemokines: a new classification system and their role in immunity. Immunity. 2000; 12:121–127. [PubMed: 10714678]
10. Yu L, Cecil J, Peng SB, et al. Identification and expression of novel isoforms of human stromal cell-derived factor 1. Gene. 2006; 374:174–179. [PubMed: 16626895]
11. Bleul CC, Farzan M, Choe H, et al. The lymphocyte chemoattractant SDF-1 is a ligand for LESTR/fusin and blocks HIV-1 entry. Nature. 1996; 382:829–833. [PubMed: 8752280]
12. Feng Y, Broder CC, Kennedy PE, et al. HIV-1 entry cofactor: functional cDNA cloning of a seven-transmembrane, G protein-coupled receptor. Science. 1996; 272:872–877. [PubMed: 8629022]
13. Heesen M, Berman MA, Benson JD, et al. Cloning of the mouse fusin gene, homologue to a human HIV-1 cofactor. J Immunol. 1996; 157:5455–5460. [PubMed: 8955194]
14. Kucia M, Jankowski K, Reca R, et al. CXCR4-SDF-1 signalling, locomotion, chemotaxis and adhesion. J Mol Histol. 2004; 35:233–245. [PubMed: 15339043]
15. Granero-Molto F, Weis JA, Miga MI, et al. Regenerative effects of transplanted mesenchymal stem cells in fracture healing. Stem Cells. 2009; 27:1887–1898. [PubMed: 19544445]
16. Kitaori T, Ito H, Schwarz EM, et al. Stromal cell-derived factor 1/CXCR4 signaling is critical for the recruitment of mesenchymal stem cells to the fracture site during skeletal repair in a mouse model. Arthritis Rheum. 2009; 60:813–823. [PubMed: 19248097]
17. Otsuru S, Tamai K, Yamazaki T, et al. Circulating bone marrow-derived osteoblast progenitor cells are recruited to the bone-forming site by the CXCR4/stromal cell-derived factor-1 pathway. Stem Cells. 2008; 26:223–234. [PubMed: 17932420]
18. Kortesidis A, Zannettino A, Isenmann S, et al. Stromal-derived factor-1 promotes the growth, survival, and development of human bone marrow stromal stem cells. Blood. 2005; 105:3793–3801. [PubMed: 15677562]
19. Hosogane N, Huang Z, Rawlins BA, et al. Stromal derived factor-1 regulates bone morphogenetic protein 2-induced osteogenic differentiation of primary mesenchymal stem cells. Int J Biochem Cell Biol. 2010; 42:1132–1141. [PubMed: 20362069]
20. Zhu W, Boachie-Adjei O, Rawlins BA, et al. A novel regulatory role for stromal-derived factor-1 signaling in bone morphogenic protein-2 osteogenic differentiation of mesenchymal C2C12 cells. J Biol Chem. 2007; 282:18676–18685. [PubMed: 17439946]
21. Herberg S, Fulzele S, Yang N, et al. Stromal cell-derived factor-1beta potentiates bone morphogenetic protein-2-stimulated osteoinduction of genetically engineered bone marrow-derived mesenchymal stem cells in vitro. Tissue Eng Part A. 2013; 19:1–13. [PubMed: 22779446]
22. Higashino K, Viggeswarapu M, Bargouti M, et al. Stromal cell-derived factor-1 potentiates bone morphogenetic protein-2 induced bone formation. Tissue Eng Part A. 2011; 17:523–530. [PubMed: 21043834]
23. Wise JK, Sumner DR, Virdi AS. Modulation of stromal cell-derived factor-1/CXC chemokine receptor 4 axis enhances rhBMP-2-induced ectopic bone formation. Tissue Eng Part A. 2012; 18:860–869. [PubMed: 22035136]
24. Ratanavaraporn J, Furuya H, Kohara H, et al. Synergistic effects of the dual release of stromal cell-derived factor-1 and bone morphogenetic protein-2 from hydrogels on bone regeneration. Biomaterials. 2011; 32:2797–2811. [PubMed: 21257197]
25. Zhu W, Liang G, Huang Z, et al. Conditional inactivation of the CXCR4 receptor in osteoprecursors reduces postnatal bone formation due to impaired osteoblast development. J Biol Chem. 2011; 286:26794–26805. [PubMed: 21636574]
26. Herberg S, Susin C, Pelaez M, et al. Low-dose bone morphogenetic protein-2/stromal cell-derived factor-1beta cotherapy induces bone regeneration in critical-size rat calvarial defects. Tissue Eng Part A. 2014; 20:1444–1453. [PubMed: 24341891]

27. Davis DA, Singer KE, De La Luz Sierra, et al. Identification of carboxypeptidase N as an enzyme responsible for C-terminal cleavage of stromal cell-derived factor-1alpha in the circulation. Blood. 2005; 105:4561–4568. [PubMed: 15718415]
28. De La Luz Sierra, Yang M, Narazaki F, et al. Differential processing of stromal-derived factor-1alpha and stromal-derived factor-1beta explains functional diversity. Blood. 2004; 103:2452–2459. [PubMed: 14525775]
29. Marquez-Curtis L, Jalili A, Deiteren K, et al. Carboxy-peptidase M expressed by human bone marrow cells cleaves the C-terminal lysine of stromal cell-derived factor-1alpha: another player in hematopoietic stem/progenitor cell mobilization. Stem Cells. 2008; 26:1211–1220. [PubMed: 18292211]
30. Herberg S, Shi X, Johnson MH, et al. Stromal cell-derived factor-1beta mediates cell survival through enhancing autophagy in bone marrow-derived mesenchymal stem cells. PLoS ONE. 2013; 8:e58207. [PubMed: 23472159]
31. Zhang W, Ou G, Hamrick M, et al. Age-related changes in the osteogenic differentiation potential of mouse bone marrow stromal cells. J Bone Miner Res. 2008; 23:1118–1128. [PubMed: 18435580]
32. Zhang W, Yang N, Shi XM. Regulation of mesenchymal stem cell osteogenic differentiation by glucocorticoid-induced leucine zipper (GILZ). J Biol Chem. 2008; 283:4723–4729. [PubMed: 18084007]
33. Gimble JM, Robinson CE, Wu X, et al. Peroxisome proliferator-activated receptor-gamma activation by thiazolidinediones induces adipogenesis in bone marrow stromal cells. Mol Pharmacol. 1996; 50:1087–1094. [PubMed: 8913339]
34. Peister A, Mellad JA, Larson BL, et al. Adult stem cells from bone marrow (MSCs) isolated from different strains of inbred mice vary in surface epitopes, rates of proliferation, and differentiation potential. Blood. 2004; 103:1662–1668. [PubMed: 14592819]
35. Tropel P, Noel D, Platet N, et al. Isolation and characterisation of mesenchymal stem cells from adult mouse bone marrow. Exp Cell Res. 2004; 295:395–406. [PubMed: 15093739]
36. Ory DS, Neugeboren BA, Mulligan RC. A stable human-derived packaging cell line for production of high titer retrovirus/vesicular stomatitis virus G pseudotypes. Proc Natl Acad Sci U S A. 1996; 93:11400–11406. [PubMed: 8876147]
37. Herberg S, Kondrikova G, Periyasamy-Thandavan S, et al. Inkjet-based biopatterning of SDF-1beta augments BMP-2-induced repair of critical size calvarial bone defects in mice. Bone. 2014; 67:95–103. [PubMed: 25016095]
38. Ripoll CB, Bunnell BA. Comparative characterization of mesenchymal stem cells from eGFP transgenic and non-transgenic mice. BMC Cell Biol. 2009; 10:3. [PubMed: 19144129]
39. Yang Y, Schumacher A, Yang Y, et al. Monitoring bone marrow-originated mesenchymal stem cell traffic to myocardial infarction sites using magnetic resonance imaging. Magnetic resonance in medicine: official journal of the Society of Magnetic Resonance in Medicine/Society of Magn Reson Med. 2011; 65:1430–1436.
40. Day RM, Davis TA, Barshishat-Kupper M, et al. Enhanced hematopoietic protection from radiation by the combination of genistein and captopril. Int Immunopharmacol. 2013; 15:348–356. [PubMed: 23328620]
41. Christopherson KW 2nd, Hangoc G, Mantel CR, et al. Modulation of hematopoietic stem cell homing and engraftment by CD26. Science. 2004; 305:1000–1003. [PubMed: 15310902]
42. Elmshauser C, Bechtel J, Motta I, et al. Characterization of a mouse tet-on glia precursor cell line in vitro and in vivo using the electrophysiological measurement. J Physiol Paris. 2002; 96:329–338. [PubMed: 12445914]
43. Bouxsein ML, Boyd SK, Christiansen BA, et al. Guidelines for assessment of bone microstructure in rodents using micro-computed tomography. J Bone Miner Res. 2010; 25:1468–1486. [PubMed: 20533309]
44. Dempster DW, Compston JE, Drezner MK, et al. Standardized nomenclature, symbols, and units for bone histomorphometry: a 2012 update of the report of the ASBMR histomorphometry nomenclature committee. J Bone Miner Res. 2013; 28:2–17. [PubMed: 23197339]

45. Parfitt AM, Drezner MK, Glorieux FH, et al. Bone histomorphometry: standardization of nomenclature, symbols, and units. Report of the ASBMR Histomorphometry Nomenclature Committee. J Bone Miner Res. 1987; 2:595–610. [PubMed: 3455637]
46. Egan KP, Brennan TA, Pignolo RJ. Bone histomorphometry using free and commonly available software. Histopathology. 2012; 61:1168–1173. [PubMed: 22882309]
47. Katayama Y, Battista M, Kao WM, et al. Signals from the sympathetic nervous system regulate hematopoietic stem cell egress from bone marrow. Cell. 2006; 124:407–421. [PubMed: 16439213]
48. Gossen M, Bujard H. Studying gene function in eukaryotes by conditional gene inactivation. Annu Rev Genet. 2002; 36:153–173. [PubMed: 12429690]
49. Francois S, Bensidhoum M, Mouiseddine M, et al. Local irradiation not only induces homing of human mesenchymal stem cells at exposed sites but promotes their widespread engraftment to multiple organs: a study of their quantitative distribution after irradiation damage. Stem Cells. 2006; 24:1020–1029. [PubMed: 16339642]
50. Wang L, Liu Y, Kalajzic Z, et al. Heterogeneity of engrafted bone-lining cells after systemic and local transplantation. Blood. 2005; 106:3650–3657. [PubMed: 16081694]
51. Mouiseddine M, Francois S, Semont A, et al. Human mesenchymal stem cells home specifically to radiation-injured tissues in a non-obese diabetes/severe combined immunodeficiency mouse model. Br J Radiol. 2007; 80:S49–S55. [PubMed: 17704326]
52. Chapel A, Bertho JM, Bensidhoum M, et al. Mesenchymal stem cells home to injured tissues when co-infused with hematopoietic cells to treat a radiation-induced multi-organ failure syndrome. J Gene Med. 2003; 5:1028–1038. [PubMed: 14661178]
53. Ponomaryov T, Peled A, Petit I, et al. Induction of the chemokine stromal-derived factor-1 following DNA damage improves human stem cell function. J Clin Invest. 2000; 106:1331–1339. [PubMed: 11104786]
54. Thanik VD, Chang CC, Lerman OZ, et al. Cutaneous low-dose radiation increases tissue vascularity through upregulation of angiogenic and vasculogenic pathways. J Vasc Res. 2010; 47:472–480. [PubMed: 20431296]
55. Dominici M, Rasini V, Bussolari R, et al. Restoration and reversible expansion of the osteoblastic hematopoietic stem cell niche after marrow radioablation. Blood. 2009; 114:2333–2343. [PubMed: 19433859]
56. Bastianutto C, Mian A, Symes J, et al. Local radiotherapy induces homing of hematopoietic stem cells to the irradiated bone marrow. Cancer Res. 2007; 67:10112–10116. [PubMed: 17974951]
57. Zong ZW, Cheng TM, Su YP, et al. Crucial role of SDF-1/CXCR4 interaction in the recruitment of transplanted dermal multipotent cells to sublethally irradiated bone marrow. J Radiat Res. 2006; 47:287–293. [PubMed: 16974072]
58. Lataillade JJ, Clay D, Dupuy C, et al. Chemokine SDF-1 enhances circulating CD34(+) cell proliferation in synergy with cytokines: possible role in progenitor survival. Blood. 2000; 95:756–768. [PubMed: 10648383]
59. Grafte-Faure S, Leveque C, Ketata E, et al. Recruitment of primitive peripheral blood cells: synergism of interleukin 12 with interleukin 6 and stromal cell-derived FACTOR-1. Cytokine. 2000; 12:1–7. [PubMed: 10623435]
60. Drury LJ, Ziarek JJ, Gravel S, et al. Monomeric and dimeric CXCL12 inhibit metastasis through distinct CXCR4 interactions and signaling pathways. Proc Natl Acad Sci U S A. 2011; 108:17655–17660. [PubMed: 21990345]
61. Takekoshi T, Ziarek JJ, Volkman BF, et al. A locked, dimeric CXCL12 variant effectively inhibits pulmonary metastasis of CXCR4-expressing melanoma cells due to enhanced serum stability. Mol Cancer Ther. 2012; 11:2516–2525. [PubMed: 22869557]
62. Reiter E, Ahn S, Shukla AK, et al. Molecular mechanism of beta-arrestin-biased agonism at seven-transmembrane receptors. Annu Rev Pharmacol Toxicol. 2012; 52:179–197. [PubMed: 21942629]
63. Martin-Badosa E, Amblard D, Nuzzo S, et al. Excised bone structures in mice: imaging at three-dimensional synchrotron radiation micro CT. Radiology. 2003; 229:921–928. [PubMed: 14657323]

64. Green DE, Adler BJ, Chan ME, et al. Devastation of adult stem cell pools by irradiation precedes collapse of trabecular bone quality and quantity. J Bone Miner Res. 2012; 27:749–759. [PubMed: 22190044]

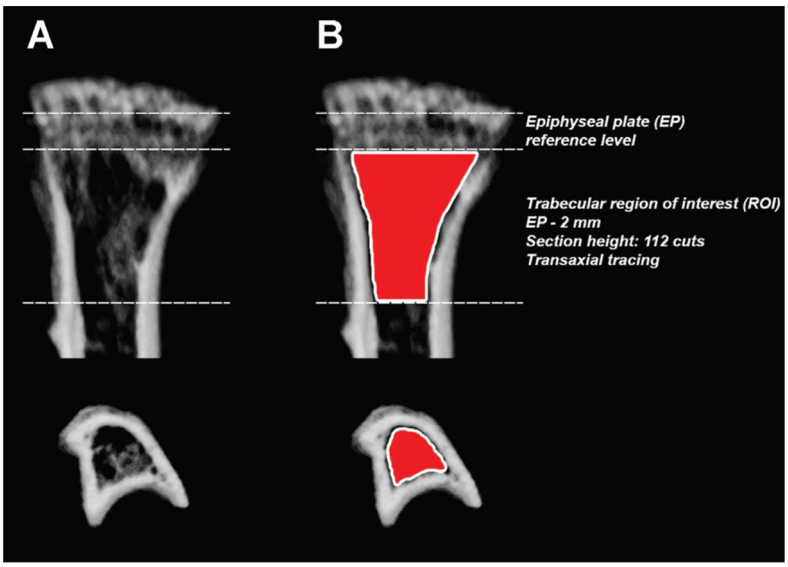

Figure 1.

Schematic of the region of interest (ROI) for 3-D trabecular bone morphometric analysis using μCT. (A) Coronal and transverse views of a representative proximal tibia. (B) Using the epiphyseal plate (EP) as a reference level, quantitative analyses of trabecular bone morphometric parameters were performed using an ROI (delineated by the Skyscan CTAn software tool using freehand drawing depicted in red) starting immediately beyond the EP and extending 112 cuts/2 mm distally by transaxial tracing.

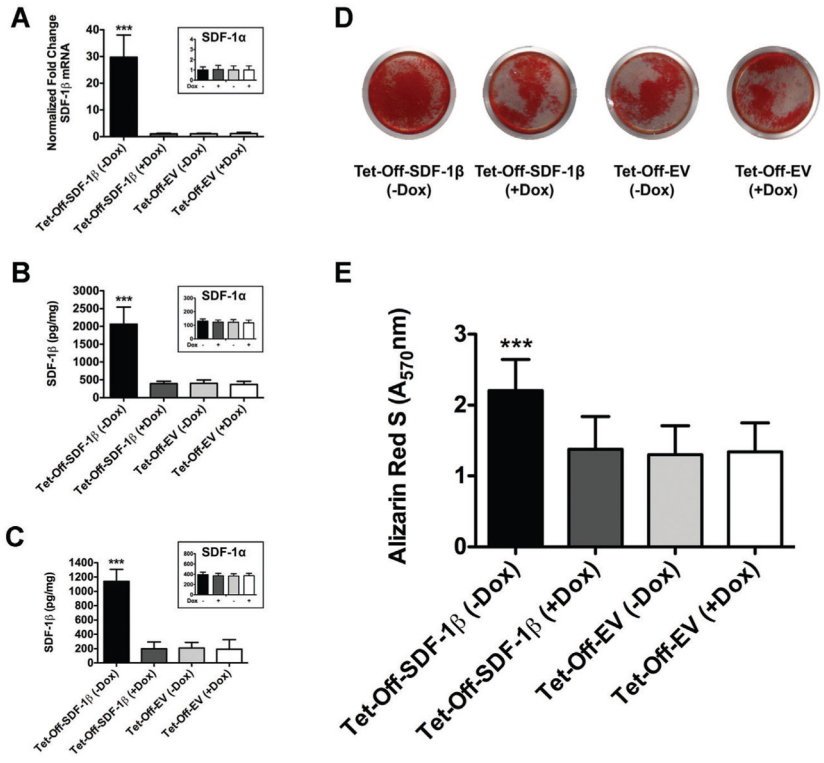

Figure 2.

SDF-1β mRNA and protein levels in Tet-Off-SDF-1β BMSCs are significantly increased relative to controls, which enhances BMSC osteogenic differentiation in vitro. (A) Normalized SDF-1β mRNA, (B) intracellular SDF-1β protein, and (C) extracellular SDF-1β protein levels. Insets show normalized SDF-1α mRNA and protein levels, respectively controls (24 h, ± 100 ng/ml Dox). (D) Representative Alizarin Red S (ARS)-stained wells (21 days, ± 100 ng/ml Dox). (E) Colorimetric quantification of extracted ARS at 570 nm. Tet-Off-SDF-1β or Tet-Off-EV BMSCs (± Dox) (***p <0.0001 Tet-Off-SDF-1β (−Dox) vs. Tet-Off-SDF-1β (+Dox) or Tet-Off-EV (±Dox), n = 3 per group).

Figure 3.

SDF-1β promotes BMSC-mediated new bone formation following direct tibial transplantation in irradiation-preconditioned animals. Representative 3-D reconstructions of μCT images 4 weeks post-transplantation (side, coronal, and transverse views; ROI: starting immediately beyond the epiphyseal plate and extending 2 mm distally by transaxial tracing for 112 cuts). (A) Vehicle-transplanted (right) tibiae. (B) Tet-Off-SDF-1β (−Dox), C) Tet-Off-SDF-1β (+Dox), and D) Tet-Off-EV BMSC-transplanted (left) tibiae at 1.32×10^7 cells/ml (n = 5/Tet-Off-SDF-1β (−Dox); n = 5/Tet-Off-SDF-1β (+Dox); n = 10/Tet-Off-EV).

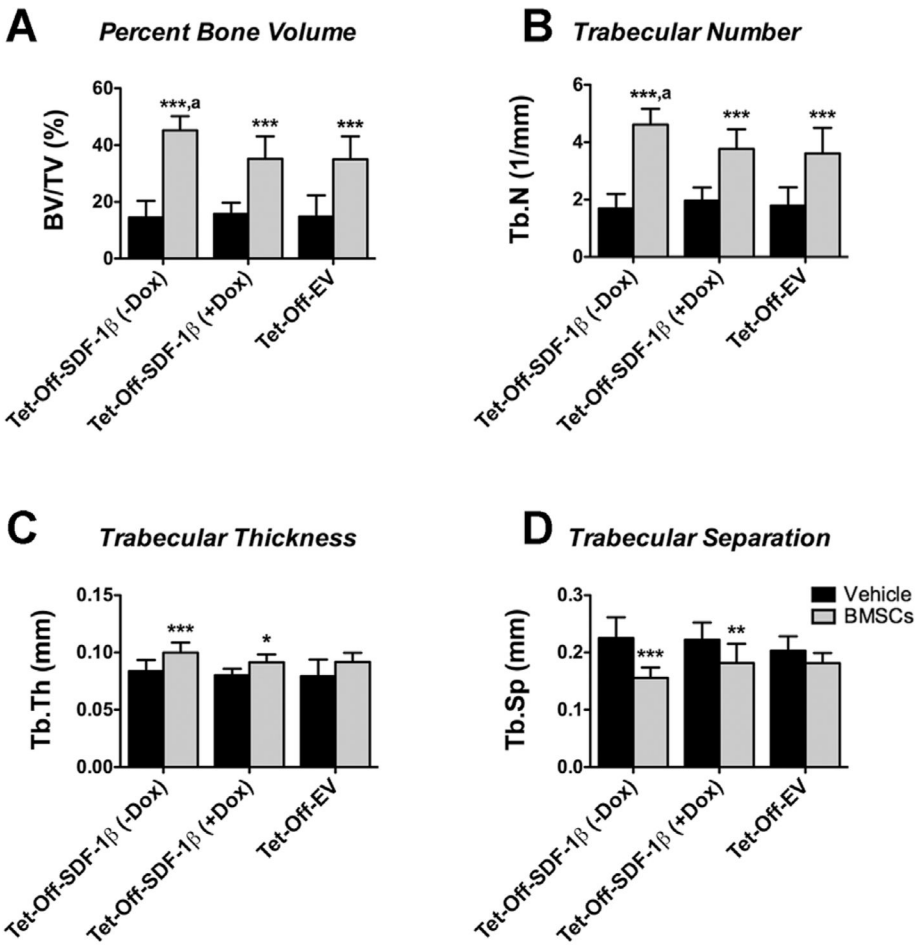

Figure 4.

SDF-1β significantly increases 3-D bone morphometric parameters following BMSC tibial transplantation in irradiation-preconditioned recipients. 3-D bone morphometric paratmeters of the proximal tibia marrow space 4 weeks post-transplantation (ROI: starting immediately beyond the epiphyseal plate and extending 2 mm distally by transaxial tracing for 112 cuts). (A) Percent bone volume (BV/TV), (B) trabecular number (Tb.N), (C) trabecular thickness (Tb.Th), and (D) trabecular separation (Tb. Sp). Vehicle- and Tet-Off-SDF-1β (± Dox) or Tet-Off-EV BMSC-transplanted tibiae at 1.32×10^7 cells/ml (*p <0.05, **p <0.01, ***p <0.0001 BMSC-transplanted vs. vehicle controls; [a]p <0.05 Tet-Off-SDF-1β (−Dox) vs. Tet-Off-SDF-1β (+Dox) or Tet-Off-EV, n = 5/Tet-Off-SDF-1β (−Dox); n = 5/Tet-Off-SDF-1β (+Dox); n = 10/Tet-Off-EV).

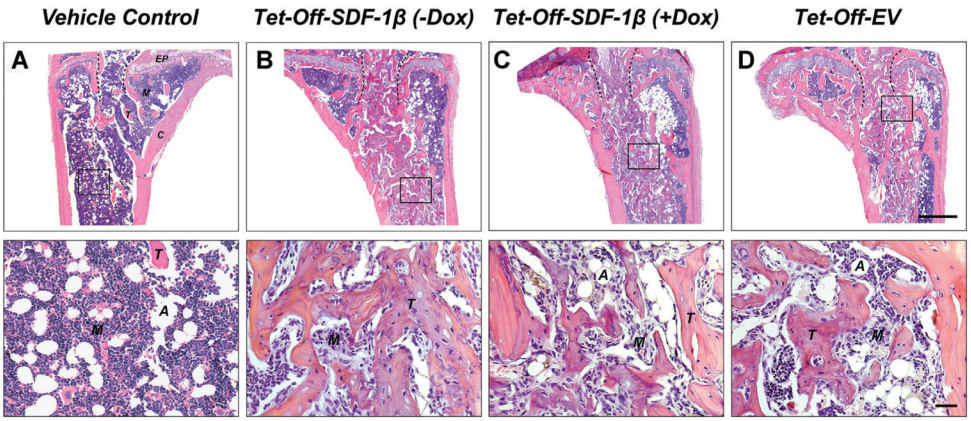

Figure 5.

SDF-1β promotes BMSC-mediated new bone formation following direct tibial transplantation in irradiation-preconditioned animals. Representative H&E-stained coronal sections (through the center of the diaphysis) of the proximal tibia marrow space 4 weeks post-transplantation (ROI: starting immediately beyond the epiphyseal plate and extending 2 mm distally). (A) Vehicle-transplanted (right) tibiae. (B) Tet-Off-SDF-1β (−Dox), (C) Tet-Off-SDF-1β (+Dox), and (D) Tet-Off-EV BMSC-transplanted (left) tibiae at 1.32×10^7 cells/ml (EP: epiphyseal plate, A: adipocyte, M: marrow, T: trabecular bone, C: cortical bone, dashed lines: outline of needle track, 2.5×, bar 500 μm, 20×, bar 20 μm, *n* = 5/Tet-Off-SDF-1β (−Dox); *n* = 5/Tet-Off-SDF-1β (+Dox); *n* = 10/Tet-Off-EV).

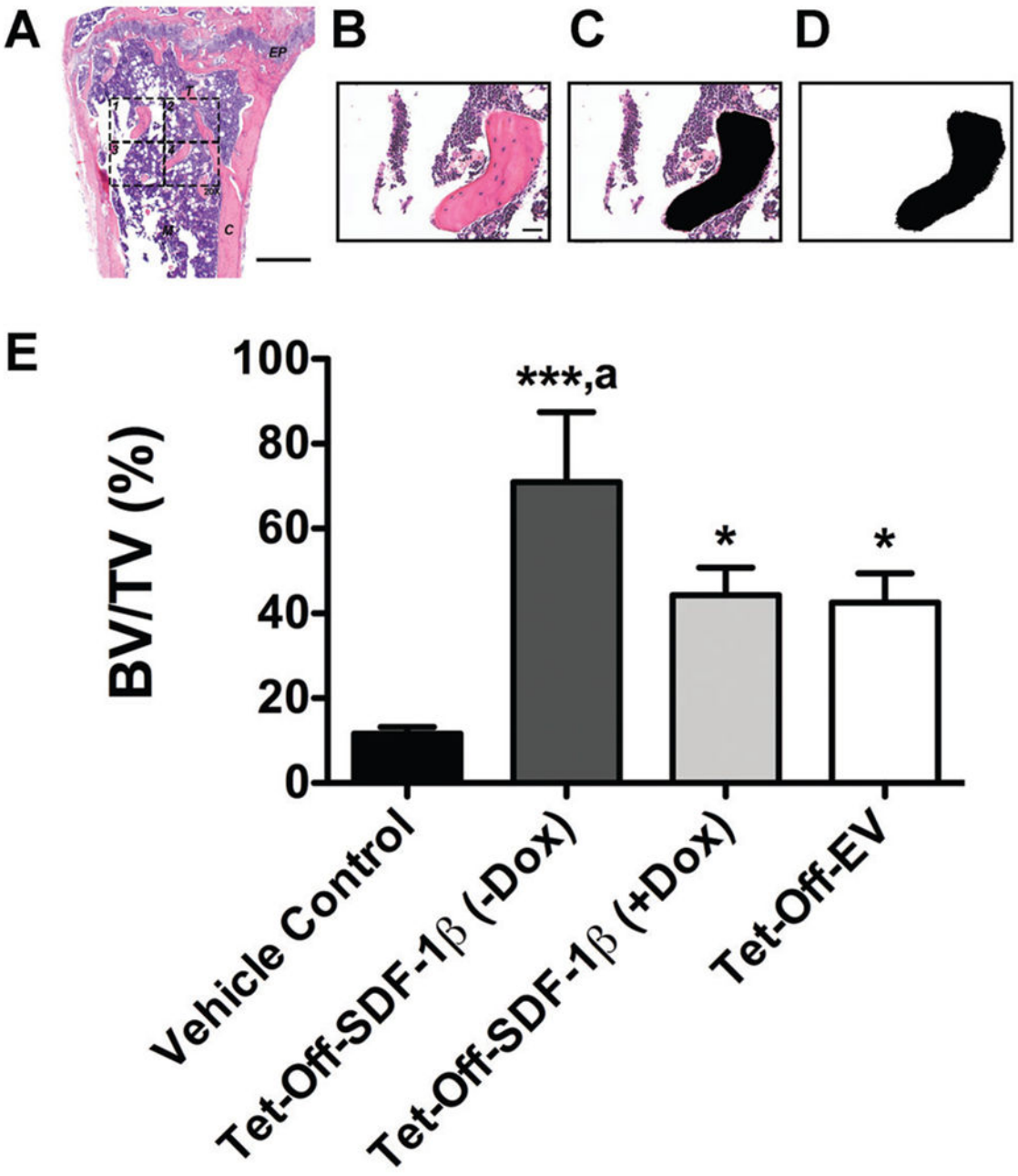

Figure 6.

SDF-1β significantly increases bone area by histomorphometry following BMSC tibial transplantation in irradiation-preconditioned recipients. The standard 2-D bone histomorphometric parameter BV/TV was assessed in the proximal tibiae 4 weeks post-transplantation. (A) Overview of a representative H&E-stained coronal section through the center of the diaphysis (EP: epiphyseal plate, M: marrow, T: trabecular bone, C: cortical bone, 2.5×, bar 500 μm). The 876.9 × 657.1 μm rectangular ROI (20×, bar 20 μm, 1388 × 1040 pixels per image, 576211.68 μm^2 or 0.58 mm^2 combined total area in 4 identical quadrants) is outlined in dashed lines. (B) One H&E-stained central coronal section 20X

ROI quadrant. (C) The same 20X ROI depicting bone tissue in black (Photo-shop wand tool, tolerance: 10). (D) Final black-and-white image mask of the 20X ROI showing bone tissue in black and all other tissue in white. Using ImageJ, the entire image area was calculated as tissue area (T.Ar) and the black-colored area was summarized as bone area (B.Ar; default ImageJ wand tool) to calculate BV/TV. Per definition, BV/TV is numerically identical with the corresponding area/area ratio B.Ar/T.Ar. E) BV/TV in vehicle- and Tet-Off-SDF-1β (±Dox) or Tet-Off-EV BMSC-transplanted tibiae at 1.32×10^7 cells/ml (*p <0.05, ***p <0.0001 BMSC-transplanted vs. vehicle controls; [a]p <0.05 Tet-Off-SDF-1β (−Dox) vs. Tet-Off-SDF-1β (+Dox) or Tet-Off-EV, n = 3 animals per group).

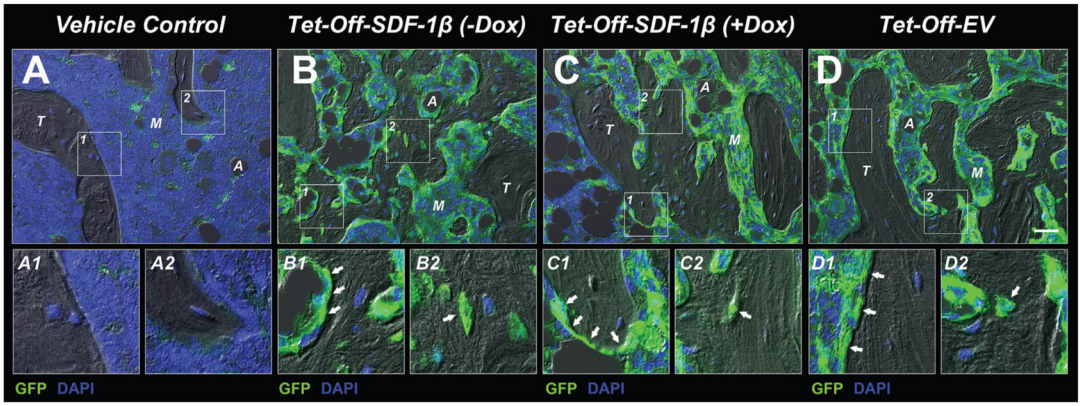

Figure 7.

SDF-1β promotes BMSC-mediated new bone formation following direct tibial transplantation in irradiation-preconditioned animals. Representative combined DIC/fluorescence micrographs of the proximal tibia marrow space (coronal sections through the center of the diaphysis) 4 weeks post-transplantation. (A) Vehicle-transplanted (right) tibiae. (B) Tet-Off-SDF-1β (−Dox), (C) Tet-Off-SDF-1β (+Dox), and D) Tet-Off-EV BMSC-transplanted (left) tibiae at 1.32×10^7 cells/ml. A-D1,2) GFP-positive cells lining trabecular structures and embedded in the bone matrix (arrows) (A: adipocyte, M: marrow, T: trabecular bone, 20X, bar 20 μm, GFP = green, DAPI = blue, *n* = 5/Tet-Off-SDF-1β (−Dox); *n* = 5/Tet-Off-SDF-1β (+Dox); *n* = 10/Tet-Off-EV).

Table 1

Oligonucleotide Primer Sequences for qRT-PCR

Gene		Sequence (5′–3′)	Product Size	Accession Number
SDF-1β	Fwd	GCTGAAGAACAACAACAGACAAGT	98	NM_013655
	Rev	CTCACATCTTGAGCCTCTTGTTTA		
SDF-1α	Fwd	GTGAGAACATGCCTAGATTTACCC	105	NM_021704
	Rev	ATAGGACTCAGGGACAATTACCAA		
Housekeeping				
β-Actin	Fwd	TGACAGACTACCTCATGAAGATCC	103	NM_007393
	Rev	ACATAGCACAGCTTCTCTTTGATG		